

MODELING A COMPOSITE REINFORCED WITH SHORT ALFA FIBERS TO DETERMINE ITS FATIGUE AND STRUCTURAL HOMOGENIZATION

A. Nour,^{1*} H. Mechakra,¹ B. Benkoussas,¹ I. Tawfiq,² A. T. Settet,¹ and R. Renane³

Keywords: Mori–Tanaka model, Eshelby tensor, Alfa fibers.

The fatigue and homogenization of polypropylene reinforced with untreated and chemically treated short Alfa fibers were investigated using a modified Mori–Tanaka model. The polypropylene with chemically treated fibers showed a higher resistance than that with untreated ones. Cylindrical fibers with elliptical cross sections were used in experiments. Their mechanical characteristics were determined by the inverse method.

1. Introduction

The fatigue behavior of vegetal-fiber composites has been investigated rarely, and even less attention has been given to composite materials reinforced with Alfa fibers. Towo and Ansell [1, 2] studied the fatigue of sisal/epoxy and sisal/polyester composites. The $S-N$ curves were presented for reinforced composites with untreated sisal fibers and sisal fibers treated with 0.06 NaOH. The sisal/epoxy composites showed a longer fatigue life than the sisal/polyester ones. In addition, the effect of the chemical treatment on the fatigue life was more significant for the sisal/polyester reinforced composites. Silva et al. [3] identified the tensile fatigue behavior of cement composites reinforced with long aligned sisal fibers. The fatigue behavior was examined in terms of stress versus the number of cycles and the stress–strain hysteresis of the composites. Elouaer et al. [4] studied the fatigue response of different varieties of composites with an injected hemp reinforcement. The authors found that the fatigue strength of hemp/PP was higher than that of hemp/CP. Similarly, Reis et al. [5] studied the flexural behavior of manually manufactured hybrid laminated composites with a natural hemp fiber/

1Dynamics of Engines and Vibroacoustic Laboratory, F.S.I., M.B. Boumerdes University, Algeria

2Laboratoire QUARTZ(EA7393), Supmecca, 3 rue de Fernand Hainaut, 93407 Saint-Ouen Cedex, France

3Université Saad Dahlab, département d’Aéronautique, Blida, Algérie

*Corresponding author; tel./fax: +213 24913099; e-mail: abdelkader_nour@hotmail.fr

polypropylene core and two glass fiber/polypropylene surface layers, one on each side of specimen. Thwe and Liao [6] studied the resistance of a bamboo-fiber-reinforced polypropylene composite (BFRP) and a hybrid bamboo- and glass-fiber-reinforced polypropylene composite (BGRP) to hygrothermal aging and fatigue under cyclic tensile loads. Ferreira et al. [7] studied the fatigue of composite adhesive lap joints. The adhesive used was a Bostik 7452 (Rubber and Plastics Grade) ethyl cyanoacrylate. Gassan [8] studied the fatigue of flax/epoxy and flax/polyester composites in comparison with that of composites reinforced with jute fibers. The results showed that the damping properties of flax/epoxy were better than those of jute/epoxy ones. Miraoui and Hassis [9] developed a mechanical model for vegetal-fiber-reinforced composite materials to determine the optimization parameters necessary for maximizing the stress in vegetal fibers. Ferreira et al. [10] studied short-vegetal-fiber-reinforced HDPE treated with electron beam radiation. Fotouh et al. [11] studied the fatigue behavior of hemp-fiber-reinforced HDPE composites. A model was developed to predict the fatigue behavior of the natural-fiber composites at different fiber fractions and fatigue stress ratios. Moraes et al. [12] studied the effect of loading frequency on the fatigue behavior of a coir-fiber-reinforced PP composite.

Regarding homogenization, Ghossein and Lévesque [13] studied the evaluation of analytical homogenization models for the case of randomly distributed and oriented ellipsoidal-fiber-reinforced composites. D. Notta-Cuvier et al. [14] focused on modeling the behavior of short-fiber-reinforced composites. Willoughby et al. [15] modeled a composite material with a fiber reinforcement. An asymptotic homogenization method and an approach intended to represent a macroscopically random material were used. Ma and Hu [16] developed a general micromechanical method for a micropolar composite with ellipsoidal fibers. The influence of both the shape and size of the fibers were analyzed by the method proposed. In their research work, Sobhani Aragh et al. [17] used an equivalent continuum model based on the Eshelby–Mori–Tanaka approach to estimate a constitutive law for an elastic isotropic medium (matrix) with oriented straight carbon nanotubes (CNTs).

John and Anandjiwala [18] used a natural-fiber surface treatment method to reinforce composite materials by improving their interfacial bonding and increasing their strength. A. Bessadok et al. [19] studied the effects of chemical treatments with maleic anhydride, styrene, acrylic acid, and acetic anhydride on Alfa-fiber/unsaturated polyester composites. Furthermore, Alix et al. [20] studied the behavior of flax fibers chemically modified by silane and styrene. Lastly, Arrakhiz et al. [21, 22] determined the mechanical properties of different composite materials with chemically treated Alfa fibers.

The present study focuses on the fatigue behavior of a composite material with Alfa fibers and optimization of their chemical treatment to enhance its static mechanical characteristics (Mechakra et al. [23]); an improved Mori–Tanaka model based on the Eshelby stress tensor and an inverse method were used to determine the mechanical characteristics of the composite.

2. Fatigue test

The tests were conducted on a Zwick fatigue testing machine with a maximum load of 250 kN. All experimental data obtained were stored on an acquisition card. The tests were conducted at a frequency of 1 Hz with amplitude $\Delta F/2$ and load ratio $R = \sigma_{\min}/\sigma_{\max} = 0.1$. The choice of such a low frequency allowed us to avoid any side effect mainly due to self-heating of the material. All tests were conducted at room temperature [4]. The specimens were subjected to the load ratios of 65, 75, and 85% of the maximum load F_{\max} .

The aim of the fatigue tests was to found the $S-N$ curves, defining the lifetime of the material at a given load.

On the semi-logarithmic scale, the $S-N$ curve can be given by a linear regression of the form [4]

$$r = A - B \log(N_f), \quad (1)$$

where r is the load level ratio applied, A is material constant, B is slope of the endurance curve, and N_f is the number of cycles at break.

The form of Eq. (1) allowed us to better visualize the fatigue of the composites (polypropylene with treated and untreated short Alfa fibers) studied according to the slope (Table 1).

TABLE 1. Values of A and B used

Material	σ_{\max}	A	B
PP/Alfa-UT-30%	22.46±0.58	132.28	14.79
PP/Alfa-T48h-30%	23.27±0.21	126.72	12.45
PP/Alfa-T24h-30%	24.39±0.54	135.37	13.92

σ_{\max} — the maximum stress determined at monotonous extension with a rate of 2 mm/min.

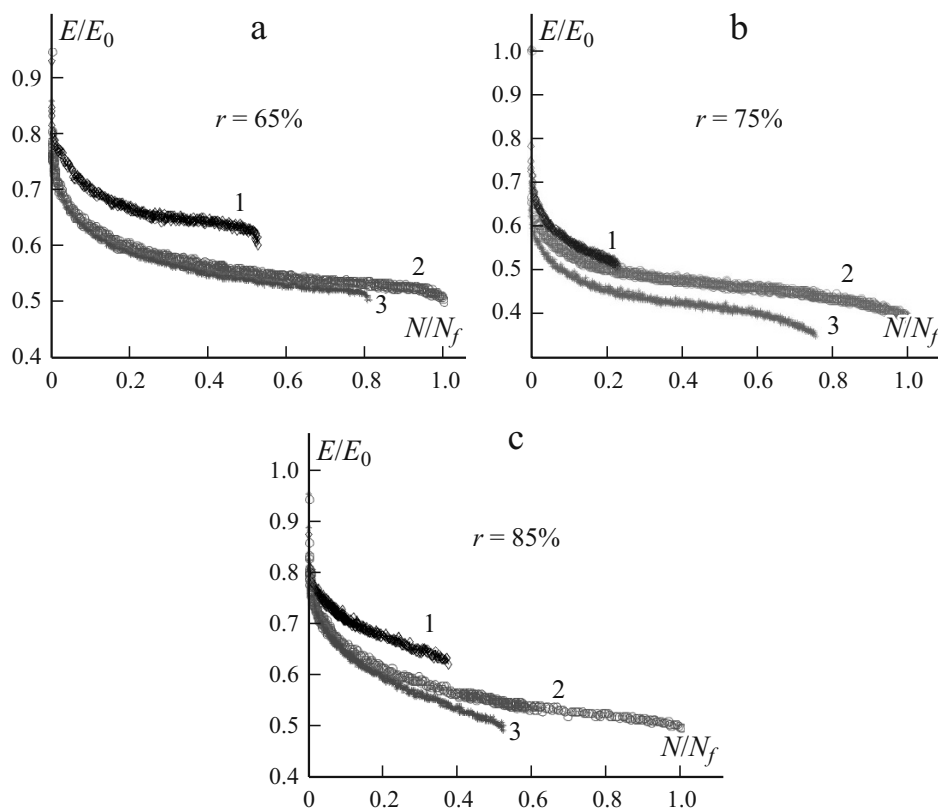


Fig. 1. Rigidity loss of polypropylene composites with untreated fibers (1) and Alfa fibers treated for 24 (2) and 48 (h).

2.1. Fatigue mechanism

Three different load ratios ($r = 65, 75$, and 85%) were used to investigate the evolution of rigidity of the materials, defined as the current rigidity E divided by the initial rigidity at the first loading cycle, E_0 , with respect to the number of cycles at break [24].

An intermediate applied load $r = 65\%$ UTS was used (Fig. 1) to validate the experimental mechanical characteristics and the effect of chemical treatment in static tests [23].

The polypropylene with Alfa fibers (treated for 24 and 48 h) exhibited a better fatigue resistance than the polypropylene with untreated ones. The residual rigidity of the composites with fibers chemically treated for 24 and 28 h was higher than of the composite with untreated fibers: by 56 and 52%, respectively, at the load $r = 65\%$ UTS (Fig. 1a); by 44.2 and 36.5%,

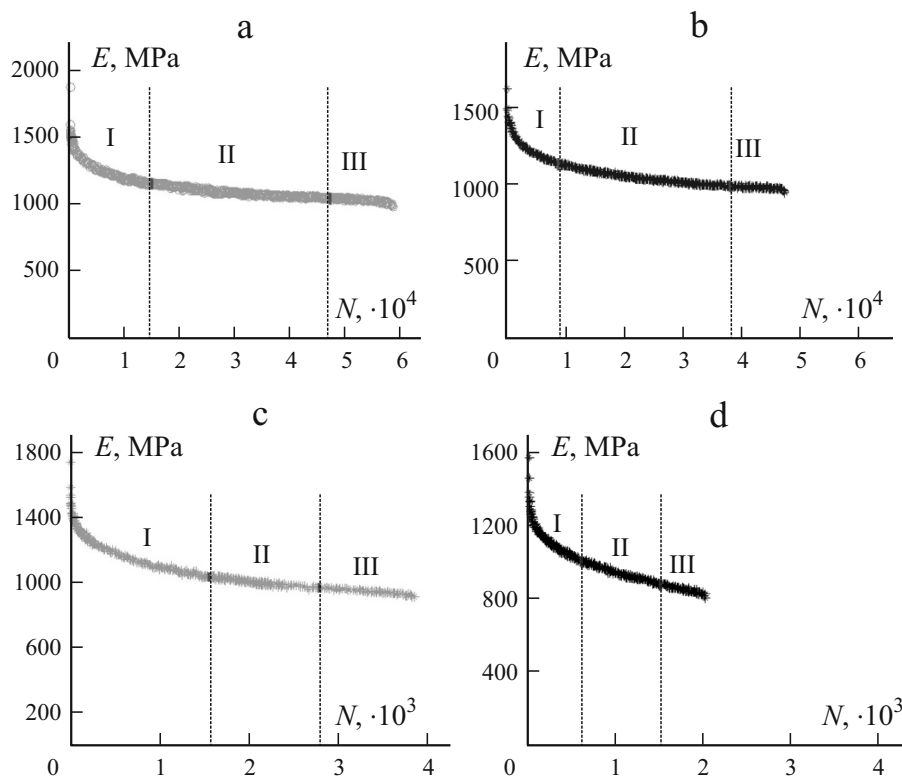


Fig. 2. Development of fatigue process in composites with fibers treated for 24 (a, c) and 48 h (b, d) at 65 (a, b) and 85% UTS (c, d).

respectively, at $r = 75\%$ UTS (Fig. 1b); by 57 and 48%, respectively, at $r = 85\%$ UTS (Fig. 1c). In addition, at $r = 85\%$ UTS, the residual strength of the composite with fibers treated for 24 h was higher than that with fibers treated for 48 h.

The fatigue strength of the composite with untreated fibers was 65% of that in the case of treated fibers. This can be explained by a better adhesion bond between the polypropylene matrix and treated fibers.

2.3. Process and fatigue mechanisms

During the cyclic fatigue loadings, three phases (I, II, and III) could be observed during the evolution of Young's modulus E as a function of the number of cycles. They are illustrated in Fig. 2 for two composites, PP/Alfa-T24h and PP/Alfa-T48h, and two loading ratios, $r = 65$ and 85% of UTS.

Phase I. A considerable and rapid decrease in E , when the first cracks appeared in the matrix. This degradation is described by the initiation of damage caused by microcracks in different parts of the matrix and fiber/matrix interfaces.

Phase II. A moderate decrease in E (the longest phase), followed by a steady state with a slow evolution of damage, corresponding to the multiplication of transverse cracks. This phase is characterized by the propagation and increase of microcracks.

Phase III. An accelerated decrease in E and a rapid development of cracks and macrocracks, corresponding to the final damage and breaking.

These phases confirm the same fatigue behavior of all thermoplastic/thermoset materials reinforced with vegetal fibers, such as, e.g., the flax/epoxy and flax/polyester studied by Elouaer et al. [4].

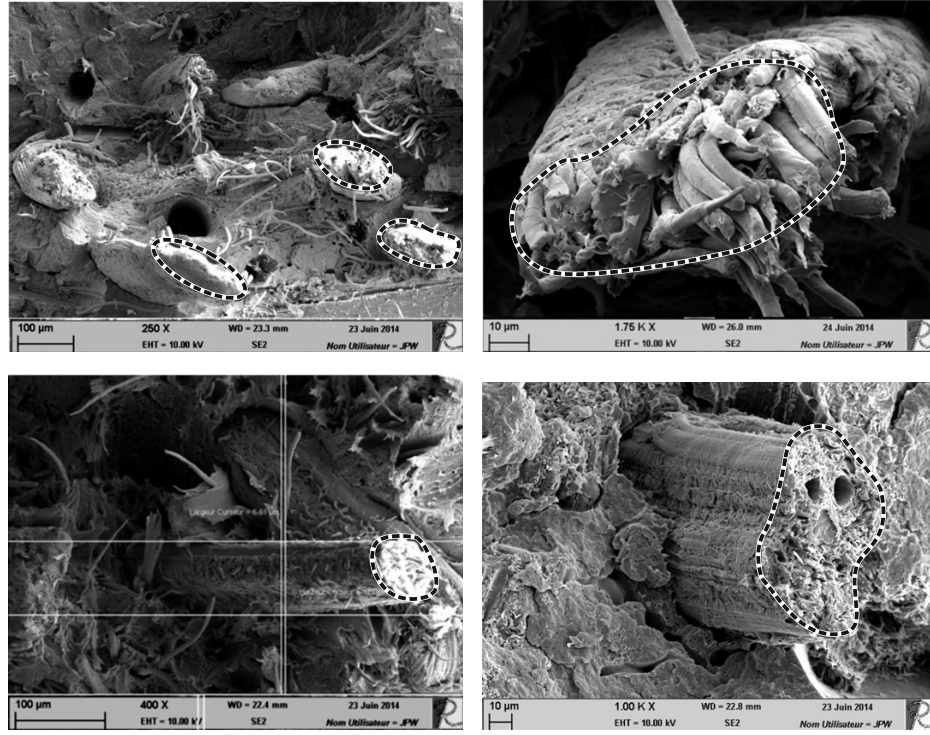


Fig. 3. Representative elementary volume (REV): SEM pictures of Alfa fibers.

3. Application of the Mori–Tanaka Model

A micromechanical calculation was performed with Matlab to obtain the numerical rigidity tensor of the composite by the Mori–Tanaka model. To ensure that the calculation run smoothly in the case of PP/Alfa-48h and PP/Alfa-24h composites, the model required the following information:

- the volume fraction of reinforcement and the elastic properties of each constituent (E and ν).
- The rigidity matrices of each constituent, with simplifying assumptions. The polypropylene resin and Alfa fibers were assumed to be isotropic.
- The geometry and orientation of fibers. Random orientation of the fibers in the model was assumed.

In the Mori–Tanaka model, two homogenization tensors that take into account the inclusion of the Eshelby tensor are considered:

1. The pseudotensor of localization [15]

$$\mathbf{L}^i = -[(\mathbf{C}^i - \mathbf{C}^0)\mathbf{S}_{\text{Esh}}^i + \mathbf{C}^0]^{-1}(\mathbf{C}^i - \mathbf{C}^0), \quad (2)$$

where \mathbf{C}^i is the rigidity tensor of inclusion, \mathbf{C}^0 is the rigidity tensor of matrix, and $\mathbf{S}_{\text{Esh}}^i$ is the Eshelby tensor.

2. The stiffness tensor of the equivalent homogeneous material

$$\mathbf{C}^c = \mathbf{C}^0 \left\{ \mathbf{I} + \sum_{i=1}^n f^i \mathbf{L}^i \left[\mathbf{I} + \sum_{i=1}^n f^i (\mathbf{S}_{\text{Esh}}^i - \mathbf{I}) \mathbf{L}^i \right]^{-1} \right\}^{-1}, \quad (3)$$

where \mathbf{I} is the 4th-order identity tensor, f^i is the volume fraction of inclusion, and \mathbf{L}^i is the localization tensor.

The rigidity tensor of the equivalent homogeneous material is a function of material microstructure parameters, the volume fraction of inclusions, the mechanical properties of matrix and inclusions, and the geometry of fibers. For the

case of a composite material reinforced with randomly oriented fibers, they are distributed in N families. Each of them has a particular orientation, and therefore they are considered as various phases [14, 25].

3.1. Components of Eshelby tensor

The nonzero components of the Eshelby tensor for an isotropic ellipsoidal inclusion with aspect ratio $\alpha = a_3/a_2$ are given in [15, 26]. The case of cylindrical inclusions with elliptical cross sections is considered in [16, 27].

3.1.1. Eshelby tensor: The Eshelby tensor depends on fiber geometry and the Poisson ratio of polypropylene matrix.

The fiber diameter ranged from 7.41 to 360 μm . Estimating the particular random distribution of short Alfa fibers in the composite, we determined the Representative Elementary Volume (REV) of the entire structure, which will be used in the rest of the study, calculated the Eshelby tensor, and determined fiber diameters a_1 and a_2 . These diameters were average of the areas of different random fiber cross sections. Finally, the values of the Alfa fiber were obtained from scanning electronical microscope (SEM) observations (Fig. 3) to calculate the average diameters (Fig. 4).

The Eshelby tensor, which considers that the fiber is elliptical, was modified by the shape of actual fractured specimens according to SEM observations (Fig. 3). After calculation, we obtain the Eshelby tensor

$$\mathbf{S}_{\text{Esh}} = \begin{bmatrix} 0.7050 & 0.1257 & 0.3323 & & & \\ 0.1278 & 0.7082 & 0.3344 & & & \\ 0 & 0 & 0 & & & \\ & & & 0.2508 & 0 & 0 \\ & & & 0 & 0.2492 & 0 \\ & & & 0 & 0 & 0.2952 \end{bmatrix}. \quad (4)$$

3.2. Polypropylene rigidity tensor

For the sake of simplicity, the polypropylene matrix was assumed isotropic, meaning that the amorphous phase and the crystalline phase had the same properties as the entire matrix. The rigidity tensor of resin has the form

$$\mathbf{C}^m = \begin{bmatrix} \lambda^m + 2\mu^m & \lambda^m & \lambda^m & & & \\ \lambda^m & \lambda^m + 2\mu^m & \lambda^m & & & \\ \lambda^m & \lambda^m & \lambda^m + 2\mu^m & & & \\ & & & \mu^m & 0 & 0 \\ & & & 0 & \mu^m & 0 \\ & & & 0 & 0 & \mu^m \end{bmatrix}, \quad (5)$$

Here, λ^m and μ^m are the Lamé coefficients of the PP matrix. They are determined by the relations

$$\lambda^m = \frac{\nu_m E_m}{(1 + \nu_m)(1 - 2\nu_m)} \quad \text{and} \quad \mu^m = \frac{E_m}{2(1 + \nu_m)},$$

where ν_m and E_m are Young's modulus and the Poisson ratio of the PP matrix. After calculations, we obtain the following rigidity tensor of PP:

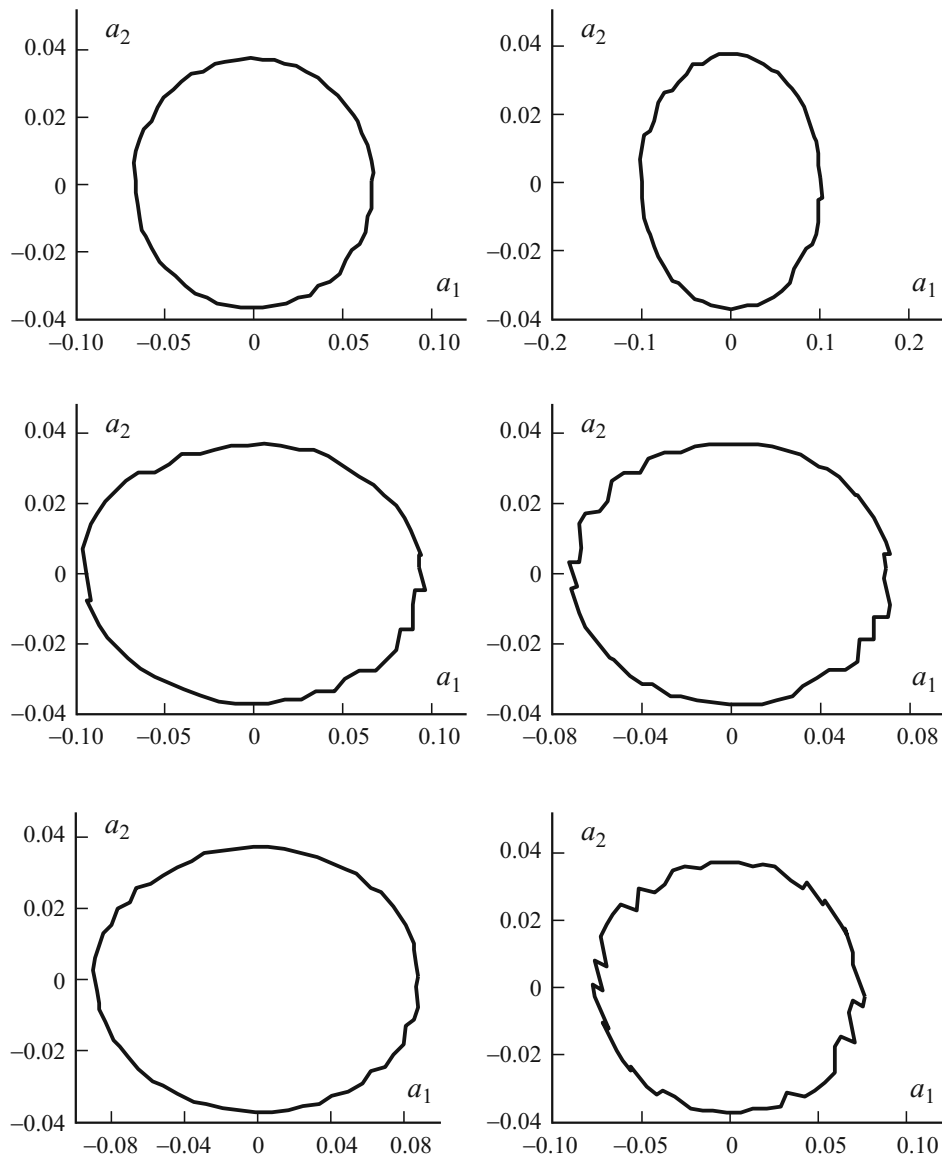


Fig. 4. Different cross sections of Alfa fibers with diameters varying between 7.41 and 360 μm .

$$\mathbf{C}^m = \begin{bmatrix} 3289.29 & 2192.86 & 2192.86 & & & \\ 2192.86 & 3289.29 & 2192.86 & & & \\ 2192.86 & 2192.86 & 3289.29 & & & \\ & & & [0] & & \\ & & & & 548.21 & 0 & 0 \\ & & & & 0 & 548.21 & 0 \\ & & & & 0 & 0 & 548.21 \end{bmatrix}. \quad (6)$$

Note that, in the analytical equations of the Mori–Tanaka model, the rigidity tensor of matrix is denoted by \mathbf{C}^0 ; in our case, it is denoted by \mathbf{C}^m .

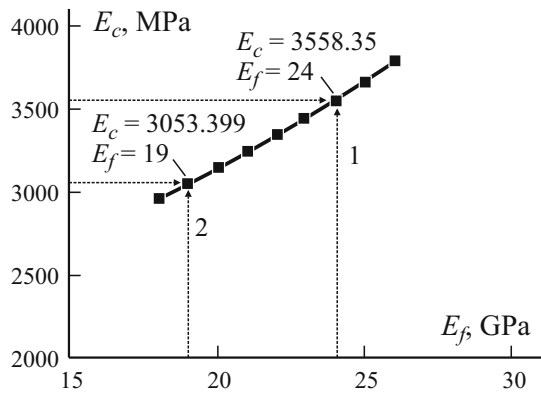


Fig. 5. Determination of Young's modulus of the Alfa fibers treated for 24 and 48h.

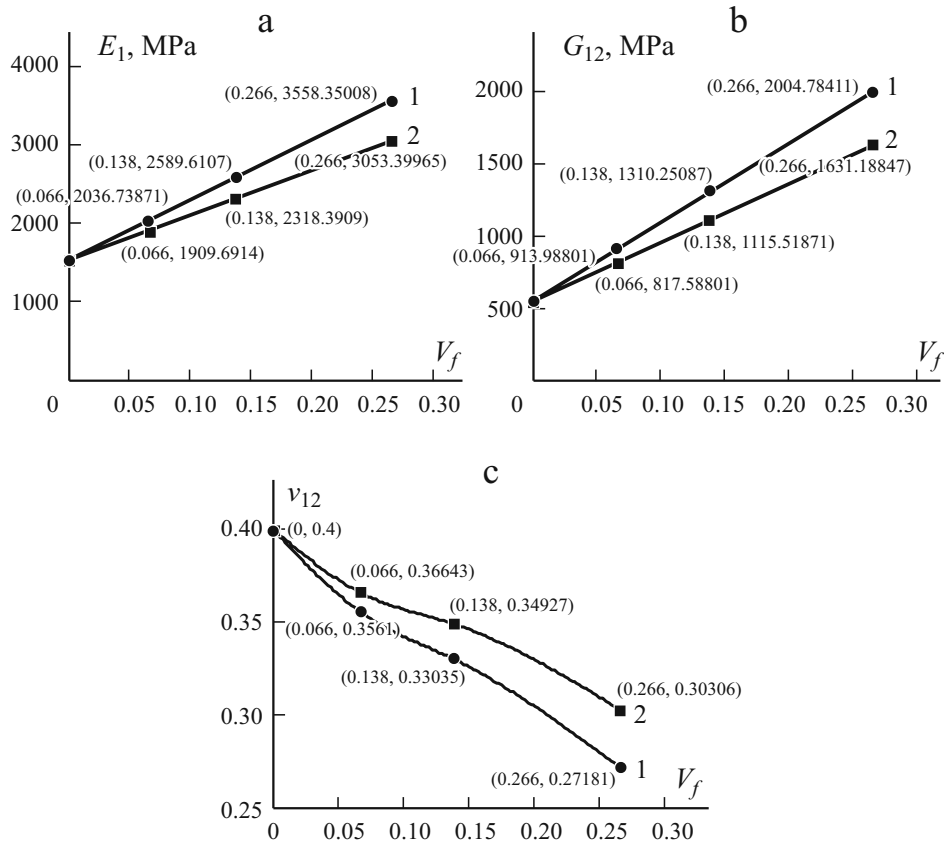


Fig. 6. E_1 (a), G_{12} (b) and ν_{12} (c) of PP/Alfa-T24h (1) and PP/Alfa t48h (2) vs. fiber volume fraction V_f .

For the modulus $E_c = 3558.35$ MPa of the PP/Alfa-T24h composite, the corresponding analytical Young's modulus of the fiber was $E_f = 24,000$ MPa and its Poisson ratio was $\nu_{12} = 0.2718$. The analytical Young's modulus $E_f = 19,000$ MPa and Poisson ratio $\nu_{12} = 0.3030$ were deduced from the same curve for the longitudinal elastic modulus $E_c = 3053.38$ MPa of the PP/Alfa composite reinforced with fibers treated for 48 h.

Thus, the elastic modulus of the Alfa fiber treated for 24h ($E_f = 24,000$ MPa) was greater than that of the Alfa fiber treated for 48 h ($E_f = 19,000$ MPa). This result seems logical and predictable, because the rigidity of the Alfa fiber treated for 24 h was higher than that of the fiber treated for 48 h [23].

4. Parametric Study

The previous numerical study allowed us to determine Young's moduli of fibers treated for 24 and 48 h. In its turn, a parametric study provided a better understanding of the effect of various fiber volume fractions on the mechanical properties of the two composite materials investigated experimentally.

4.1. Effect of fiber volume fraction V_f on Young's modulus E_1

Figure 6a presents Young's modulus vs. fiber volume fraction V_f for the PP/Alfa-T48h and PP/Alfa-T24h composite materials. A linear variation in Young's modulus is seen. The Young's moduli obtained by the numerical simulation were similar to those obtained experimentally for PP/Alfa-T48h and PP/Alfa-T24h in the previous experimental static study (see Table 2 in [23]).

4.2. Effect of fiber volume fraction V_f on the shear modulus G_{12}

The shear modulus G_{12} vs. V_f in the 2D configuration (determined numerically by the Mori–Tanaka model) given in Fig. 6b shows the same effect. Indeed, a quasi-isotropic character is observed for both materials in Figs. 6a, b.

4.3. Effect of fiber volume fraction V_f on the Poisson ratio ν_{12}

Knowing that the Poisson ratio of the composite cannot be determined experimentally, the Mori–Tanaka micromechanical model was used to evaluate it for the two composite materials in relation to the fiber volume fraction V_f . Results for both the materials are illustrated in Fig. 6c.

As is seen, the Poisson ratio decreases with growing V_f for both the PP/Alfa-T48h and PP/Alfa-T24h composites in contrast to the elastic moduli E_1 and G_{12} , which both increase.

Conclusion

The fatigue tests on composite materials made by reinforcing polypropylene with 30% of untreated and chemically treated Alfa fibers were performed to their static behavior by evaluating the mechanical characteristics experimentally. Based on the results obtained, the following conclusions were drawn.

- The PP/Alfa composite with fibers treated for 24h was the strongest material owing to a better distribution of fibers in the matrix, which agreed well with data obtained in static tests.

- A micromechanical modeling was carried out to validate the experimental results. The Mori–Tanaka model was used due to experimental difficulties in determining the mechanical characteristics of fibers parameters. Their Young's modulus was obtained using an inverse method, by varying fiber properties found from the curve describing the macroscopic elastic modulus of the composites.

- The Mori–Tanaka model, based on the Eshelby tensor, was modified to take into account the cylindrical cross section of fibers and the Poisson ratio of polypropylene matrix. An elliptical cross section of the fibers was introduced and examined using SEM observations and the fracture surfaces of composite samples.

REFERENCES

1. A. N. Towo and M. P. Ansell, "Fatigue evaluation and dynamic mechanical thermal analysis of sisal fiber–thermosetting resin composites," *Compos. Sci. Technol.*, **68**, 925-932 (2008).
2. A. N. Towo and M. P. Ansell, "Fatigue of sisal fiber reinforced composites: Constant-life diagrams and hysteresis loop capture," *Compos. Sci. Technol.*, **68**, 915-924 (2008).
3. F. A. Silva, B. Mobasher, and R. D. T. Filho, "Fatigue behavior of sisal fiber reinforced cement composites," *Mater. Sci. Eng. A*, **527**, No. 21-22, 5507-5513 (2010).
4. A. Elouaer, Z. Aboura, R. Ayad, H. Sabhi, M. L. Benzeggagh, *Suivi de l'endommagement en fatigue des composites à base de fibres végétales*, Comptes Rendus des JNC 16, Toulouse (2009).
5. P. N. B. Reis, J. A. M. Ferreira, F. V. Antunes, and J. D. M. Costa, "Flexural behaviour of hybrid laminated composites," *Composites: Part A*, **38**, No. 6, 1612-1620 (2007).
6. M. M. Thwe and K. Liao, "Durability of bamboo-glass fiber reinforced polymer matrix hybrid composites," *Compos. Sci. Technol.*, **63**, No. 3-4, 375-387 (2003).
7. J. M. Ferreira, H. Silva, J. D. Costa, and M. Richardson, "Stress analysis of lap joints involving natural fiber reinforced interface layers," *Composites: Part B*, **36**, No. 1-7, (2003).
8. J. A. Gassan, "Study of fiber and interface parameters affecting the fatigue behaviour of natural fiber composites," *Composites: Part A*, **33**, No. 3, 369-374 (2002).
9. I. Miraoui and H. Hassis, "Mechanical model for vegetal fibers-reinforced composite materials," *Physics Procedia*, **25**, 130-136 (2012).
10. M. S. Ferreira, M. N. Sartori, R. R. Oliveira, G. E. Olgun, and A. B. Moura, "Short vegetal-fiber reinforced HDPE—A study of electron-beam radiation treatment effects on mechanical and morphological properties," *Appl. Surface Sci.*, **310**, 325-330 (2014).
11. A. Fotouh, J. D. Wolodko, and M. G. Lipset, "Fatigue of natural fiber thermoplastic composites," *Composites: Part B: Eng.*, **62**, 175-182 (2014).
12. D. V. O. Moraes, R. Magnabosco, G. H. B. Donato, S. H. P. Bettini, and M. C. Antunes, "Influence of loading frequency on the fatigue behaviour of coir fiber reinforced PP composite," *Polymer Testing*, **41**, 184-190 (2015).
13. E. Ghossein and M. Lévesque, "A comprehensive validation of analytical homogenization models: The case of ellipsoidal particles reinforced composites," *Mech. of Mater.*, **75**, 135-150 (2014).
14. D. Notta-Cuvier, F. Lauro, B. Bennani, and R. Balieu, "An efficient modelling of inelastic composites with misaligned short fibers," *Int. J. Solids and Structures*, **50**, 2857-2871 (2013).
15. R. Piat, I. Tsukrov, N. Mladenov, M. Guellali, R. Ermel, T. Beck, E. Schnack, and M. J. Hoffmann, "Material modeling of the CVI-infiltrated carbon felt II Statistical study of the microstructure, numerical analysis and experimental," *Compos. Sci. Technol.*, **66**, 2769-2775 (2006).
16. H. Ma and G. Hu, "Influence of fiber's shape and size on overall," *Int. J. of Solids and Structures*, **43**, 3025-3043 (2006).
17. B. Sobhani Aragh, A. H. N. Barati, and H. Hedayati, "Eshelby–Mori–Tanaka approach for vibrational behavior of continuously graded carbon nanotube-reinforced cylindrical panels," *Composites: Part B*, **43**, 1943-1954 (2012).
18. M. J. John and R. D. Anandjiwala, "Chemical modification of flax reinforced polypropylene composites," *Composites: Part A*, **40**, 442-448 (2009).
19. A. Bessadok, S. Roudesli, S. Marais, N. Follain, and L. Lebrun, "Alfa fibres for unsaturated polyester composites reinforcement: Effects of chemical treatments on mechanical and permeation properties," *Composites: Part A*, **40**, 184-95 (2009).
20. S. Alix, L. Lebrun, C. Morvan, and S. Marais, "Study of water behaviour of chemically treated flax fibres-based composites: A way to approach the hydric interface," *Compos. Sci. Technol.*, **71**, 893-899 (2011).
21. F. Z. Arrakhiz, M. Elachaby, R. Bouhfid, S. Vaudreuil, M. Essassi, and A. Qaiss, "Mechanical and thermal properties of polypropylene reinforced with Alfa fiber under different chemical treatment," *Mater. Des.*, **35**, 318-322 (2012).
22. F. Z. Arrakhiz, M. Malha, R. Bouhfid, K. Benmoussa, and A. Qaiss, "Tensile, flexural and torsional properties of chemically treated Alfa, coir and bagasse reinforced polypropylene," *Composites: Part B*, **47**, 35-41 (2013).

23. H. Mechakra, A. Nour, S. Lecheb, and A. Chellil, "Mechanical characterizations of composite material with short Alfa fibers reinforcement," *Compos. Struct.*, **124**, 152-162 (2015).
24. W. Van Paepegem and J. Degrieck, "A new coupled approach of residual stiffness and strength for fatigue of fibre-reinforced composites." *Int. J. Fatigue*, **24**, 747-762 (2002).
25. S. Ben Brahim and R. Ben Cheikh, "Influence of fiber orientation and volume fraction on the tensile properties of unidirectional Alfa-polyester composite," *Compos. Sci. Technol.*, **67**, 140-147 (2007).
26. L. Charles, Tucker III, and E. Liang, "Stiffness predictions for unidirectional short-fiber composites: Review and evaluation," *Compos. Sci. Technol.*, **59**, 655-671 (1999).
27. F. Meraghni, F. Desrumaux, and M. L. Benzeggagh, "Implementation of a constitutive micromechanical model for damage analysis in glass mat reinforced composite structures," *Compos. Sci. Technol.*, **62**, No.16, 2087-2097 (2002).
28. G. M. Odegard, T. S. Gates, K. E. Wise, C. Park, and E. J. Siochi, "Constitutive modeling of nanotube-reinforced polymer composites," *Compos. Sci. Technol.*, **63**, No. 11, 1671-1687 (2003).